catalysts

MDPI

Article

Low-Temperature Activity and PdO-PdO_x Transition in Methane Combustion by a PdO-PdO_x/γ-Al_2O_3 Catalyst

Anil C. Banerjee [1,*], Jacqueline M. McGuire [1], Olivia Lawnick [1] and Michael. J. Bozack [2]

[1] Department of Chemistry, Columbus State University, Columbus, GA 31907, USA; mcguire_jacqueline@columbusstate.edu (J.M.M.); lawnick_olivia@columbusstate.edu (O.L.)
[2] Department of Physics, Auburn University, Auburn, AL 36849, USA; bozacmj@auburn.edu
* Correspondence: banerjee_anil@columbusstate.edu; Tel.: +1-706-569-3030

Received: 21 May 2018; Accepted: 28 June 2018; Published: 29 June 2018

Abstract: The search to discover a suitable catalyst for complete combustion of methane at low temperature continues to be an active area of research. We prepared a 5 wt % PdO-PdO_x/γ-Al_2O_3 catalyst by a modified Vortex-assisted Incipient Wetness Method. X-ray Photoelectron Spectroscopy showed that the original catalyst contained PdO (38%) and PdO_x (62%) on the surface and indicated that PdO_x originated from the interaction of PdO with the support. Scanning Transmission Electron Microscopy confirmed the catalyst had an average particle size of 10 nm and was well-dispersed in the support. The catalyst exhibited exceptional low-temperature activities with 90–94% methane conversion at 300–320 °C. The catalyst was active and stable after several catalytic runs with no signs of deactivation by steam in this narrow temperature range. However, the conversion decreased in the temperature range 325–400 °C. The surface composition changed to some extent after the reaction at 325 °C. A tentative mechanism proposes PdO_x (Pd native oxide) as the active phase and migration of oxide ions from the support to PdO and then to PdO_x during the catalytic oxidation. The high methane conversion at low temperature is attributed to the vortex method providing better dispersion, and to catalyst–support interaction producing the active phase of PdO_x.

Keywords: methane combustion; palladium native oxide; PdO_x; PdO-PdO_x/γ-Al_2O_3 catalyst; vortex; vortex-assisted incipient wetness method

1. Introduction

Methane is a greenhouse gas with a global warming potential 25 times higher than carbon dioxide. One remediation technique involves the use of catalysts to convert methane into a less harmful or shorter-lived species. Of these catalysts, palladium shows promise for conversion of methane at low temperatures, lending hope to automakers and industries using turbines powered by natural gas. While the idea of low-temperature combustion is appealing, finding a catalyst that can perform in "lean-burn" conditions has been a challenge. To date, an ideal catalyst that performs optimally under 400 °C remains undiscovered, but palladium, supported on various materials, comes close [1]. Gélin and Primet [2] conducted a comprehensive review of Pt- and Pd-supported catalysts, and reported that many researchers used alumina supports. Simplicio et al. [3] prepared a Pd catalyst on a y-alumina support using the incipient wetness method and reported 50% and 90% conversion of methane at 320 °C and 400 °C, respectively. Yoshida et al. [4] reported 60% methane conversion at 380 °C by a Pd/Al_2O_3 catalyst. Gholami and Smith [5] prepared Pd/SiO_2 catalysts by the incipient wetness method and reported 50% conversion at 550 °C and 100% at 600 °C. Goodman et al. [6] developed a Pd/γ-Al_2O_3 catalyst that converted 90% methane at 400 °C, but only

30% at 325 °C. Several researchers have also used other precursors and supports for the combustion of methane. Stefanov et al. [7] reported a Pd-Co/γ-Al_2O_3 catalyst with 70% methane conversion at 400 °C; Ercolino et al. [8] developed a Pd/Co_3O_4 catalyst on ZrO_2 open cell foam, and the catalyst converted about 90% methane at 325 °C and 100% at 400 °C. Cargnello et al. [9] used a supramolecular approach to develop a novel Pd@CeO_2/hydrophobic-Al_2O_3 core-shell catalyst that converted 50% methane at 325 °C and 100% at 400 °C. A Pd/Ceria nanocatalyst supported on alumina and prepared by the solution combustion method showed 50% activity at 300 °C and 90% at 400 °C [10]. A nanozeolite silicalite-1 coating on cordierite catalyst and a nitrogen-modified perovskite-type composite catalyst converted 90% methane at 350 °C [11,12]. Zhang et al. [13] reported a Pd catalyst on an alumina-ceria support that converted 80% methane at 320 °C and 100% at 400 °C. In a recent review, Venezia et al. [14] discussed effects of oxides on supported Pd catalysts, support-metal contributions, and distribution of the active sites.

Deactivation by steam has been reported as a major issue with supported Pd catalysts [6,15–18] particularly at temperatures above 325 °C. However, Pt/Pd bimetallic catalysts were active for methane combustion in the presence of steam [6].

The nature and identity of the active phase in Pd catalysts during methane combustion is currently under dispute [2,6,7,9,18–21]. Several researchers recognize PdO as the active phase [2,6,7,9]; some advocate for Pd [18,19], and others for the Pd to PdO ratio [20,21]. Another consideration is the possibility of the support lending its constituents to the catalytic active site during the course of the reaction [20]. For example, under some situations, the oxygen from the aluminum oxide could migrate to the palladium, forming PdO or some form of PdO_x, and/or migrate to the gas-phase molecule providing oxygen for the combustion [22]. This mechanism is underexplored and is one that this research seeks to advance evidence to support or reject.

A review of the literature on the catalytic combustion of methane indicates the development of some promising catalysts. Even though Pd/Al_2O_3 catalysts have been well-studied for methane combustion, this group of catalysts exhibit poor activities at temperatures below 325 °C. One of the objectives of our research has been to address this issue. We developed a catalyst containing PdO-PdO_x on a gamma-alumina support that showed low-temperature activity at 275–325 °C. Another objective was to identify the surface compounds and their role in catalytic activity and the reaction mechanism. We hypothesize that the active phase of the catalyst is Pd native oxide (PdO_x). We also propose a new mechanism for the catalytic reaction at lower temperatures below 325 °C involving the migration of oxide ions from PdO_x to adsorbed CH_4 and from the support (γ-Al_2O_3) to PdO to form PdO_x.

2. Results and Discussion

2.1. Catalyst Preparation

The Incipient Wetness Method (IWM) has been used extensively for the preparation of supported Pd catalysts [3,8,20,22]. As a part of the preliminary investigations, we prepared a 5% Pd/γ-Al_2O_3 catalyst by IWM and determined the Pd content (by Energy Dispersive X-ray Spectroscopy (EDS)) and activity for methane combustion. This catalyst had a total Pd content of 3.2%, indicating that the mixing of the precursor (Palladium nitrate hydrate) with the support γ-Al_2O_3 was not uniform during the small-scale preparation. The catalyst also gave a very low conversion of methane below 400 °C. These preliminary results prompted us to look for a better mixing method while using IWM. The concept of vortex mixing is to improve the dispersion of particles by applying powerful shear flows [23,24]. Vortex mixing has been used in catalytic preparation for hydrogen production [23] and for the dispersion of carbon nanotubes [24]. We developed a modified *Vortex-assisted Incipient Wetness Method* (VIWM) for preparation of the catalyst and details of this method are given in the "Materials and Methods" section. The catalyst prepared by VIWM and calcined at 500 °C showed a higher Pd content (4.3%) and much better activities at lower temperatures. The use of vortexing in conjunction with IWM helped in better mixing and dispersion of the PdO/PdO_x particles in the

support. The catalyst was calcined at three different temperatures (500 °C, 750 °C, and 900 °C) to study the effect of calcination temperature. XPS showed that the surface contained both PdO and PdO_x. However, the percentage of PdO_x was more at 500 °C and it originated from the interaction of PdO with the γ-Al_2O_3 support. The change in surface composition was more likely a calcination–surface interaction effect. The "Discussion Section" provides further details.

2.2. Catalyst Characterization

2.2.1. Scanning Transmission Electron Microscopy (STEM) and EDS Elementary Mapping

Figure 1 shows the Energy Dispersive X-ray Spectra (EDS) of the catalyst. The signals of Ti and Cu in Figure 1 are from the TEM grids and TEM sample holder. The average of the scans resulted in a 0.93 atomic percent of Pd, which corresponded to a 4.3 wt % Pd. The catalyst was prepared with a 5.0 wt % Pd loading. This shows the effectiveness of the modified Vortex-assisted Incipient Wetness method in retaining and dispersing the metal in the supported catalyst. High-angle annular dark-field Scanning transmission electron microscopy (HAADF-STEM) has been used by researchers to determine particle sizes and the particle size distribution of metal/metal oxides and support materials in catalysts [3,6,9,10] Goodman et al. [6] used HAADF-STEM images to determine the crystalline structure and metal dispersion in a Pd/γ-Al_2O_3 nanocatalyst. Cargnello et al. [9] demonstrated dispersion of Pd@CeO_2 on alumina using HAADF-STEM images and EDS mapping. Using STEM measurements, Khader et al. [10] identified Pd/CeO_2 nanocrystals of 1–50 nm in size. The STEM images and EDS maps of the catalyst are shown in Figures 2–6. HAADF-STEM images (Figure 2a, Figure 3A, Figure 4, and Figure 5a) show PdO/PdO_x as bright spots on the surface of γ-Al_2O_3 crystallites. The PdO/PdO_x crystals have an average size of 5–10 nm (Figure 4) and are well-dispersed in the support (Figure 6). Figure 5 gives the contrast HAADF and Bright-field STEM images of PdO/PdO_x and γ-Al_2O_3; these images demonstrate that the support is crystalline and contains nanosize particles. Our STEM data on average particle sizes are close to the particle size of 10 nm for a PdO/γ-Al_2O_3 catalyst [3,22] and 5 nm for a Pd-Co/γ-Al_2O_3 catalyst [7].

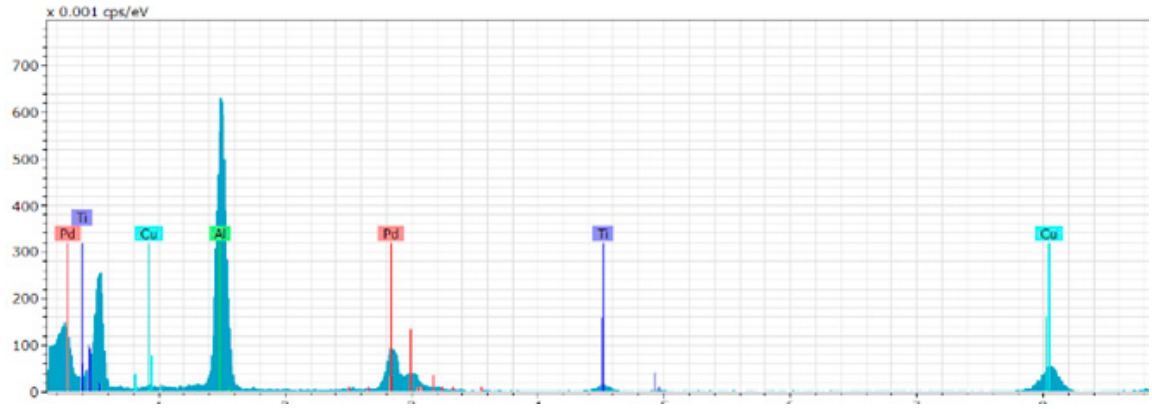

Figure 1. EDS spectra of the catalyst.

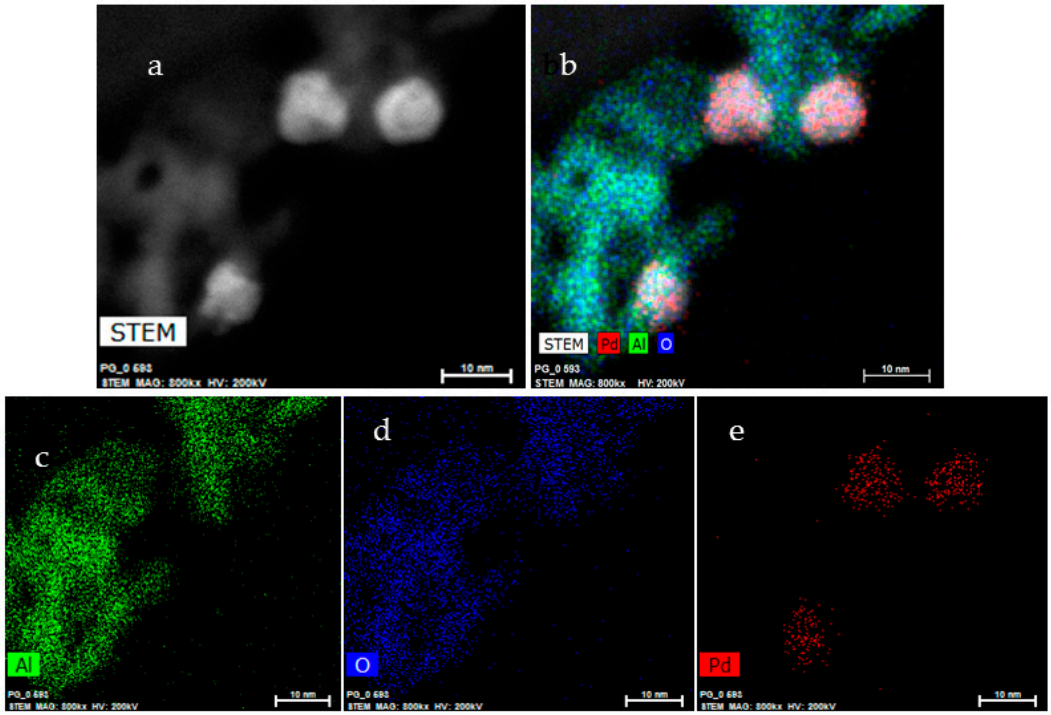

Figure 2. (**a**) STEM image; (**b**) EDS mapping; (**c**–**e**) contrast STEM images (Al, green; O, blue; Pd red). All STEM images magnification 800 kx, accelerating voltage 200kV; scale, 10 nm.

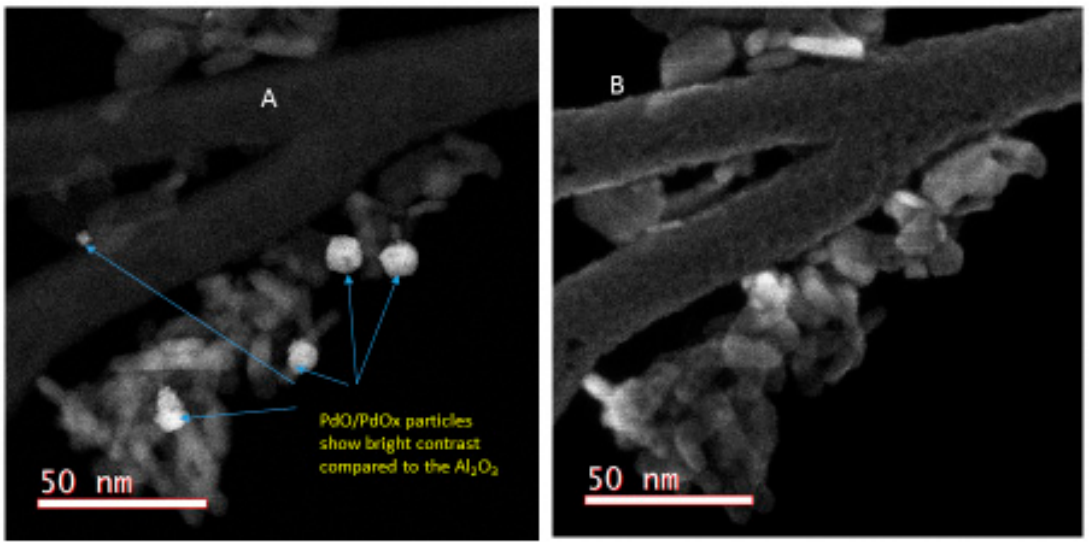

Figure 3. (**A**) HAADF STEM image from the same area of EDS mapping; (**B**) SEM image from the same area of EDS mapping.

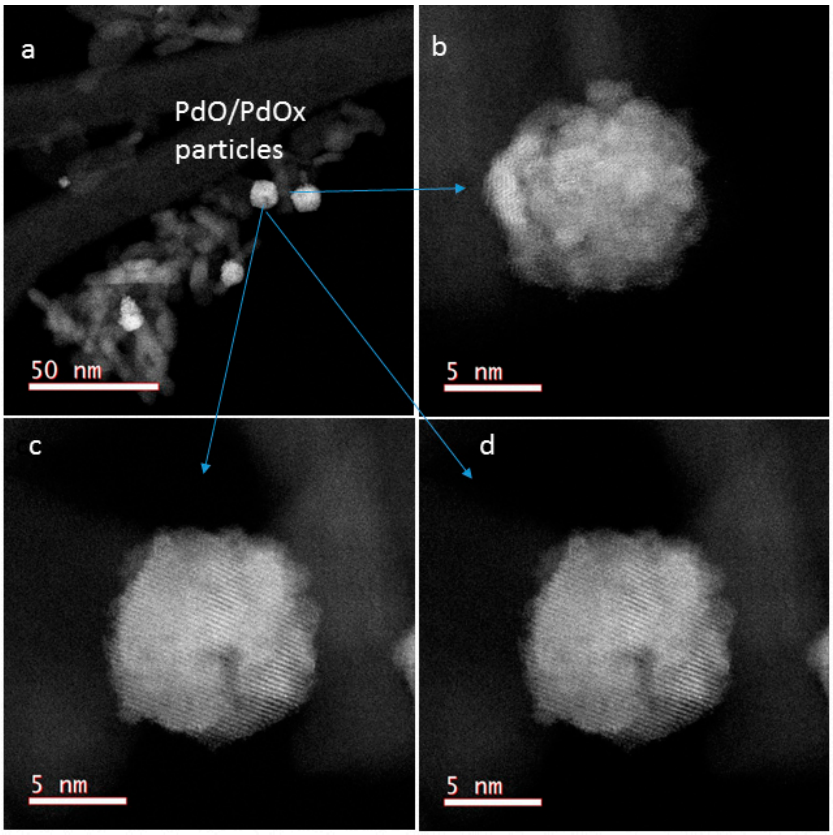

Figure 4. (**a**) HAADF-STEM images of PdO/PdO_x particles; (**b**–**d**) are magnification of the same particles; PdO/PdO_x crystals are nanoparticles of size 5–10 nm.

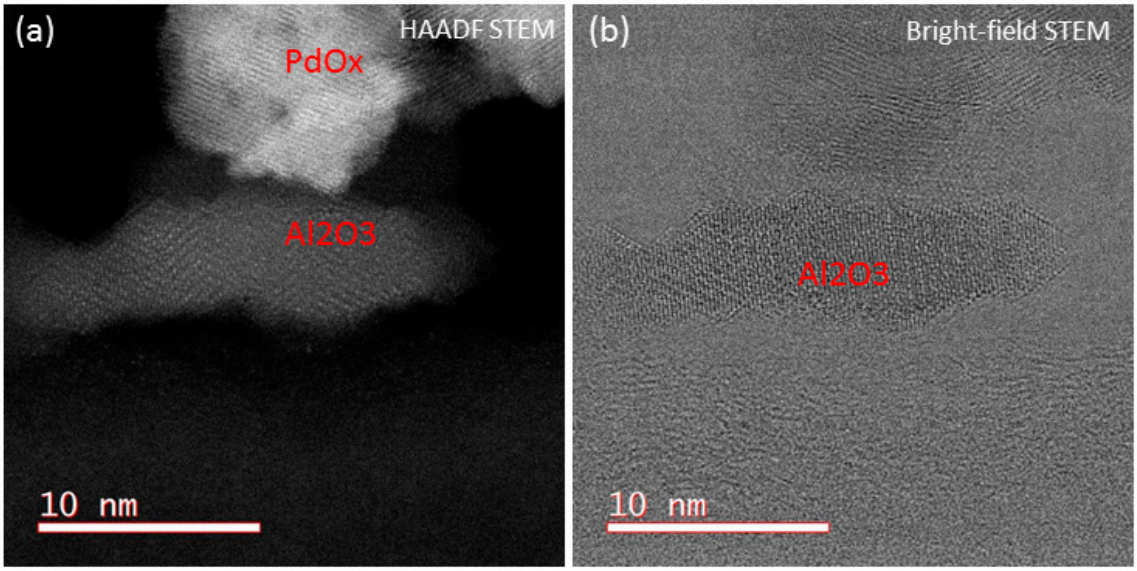

Figure 5. (**a**) z-contrast HAADF STEM image of PdO_x and γ-Al_2O_3; (**b**) phase-contrast Bright-field STEM image of PdO_x and γ-Al_2O_3. Both images are from the same area; the γ-Al_2O_3 particles are crystalline, not in amorphous phase.

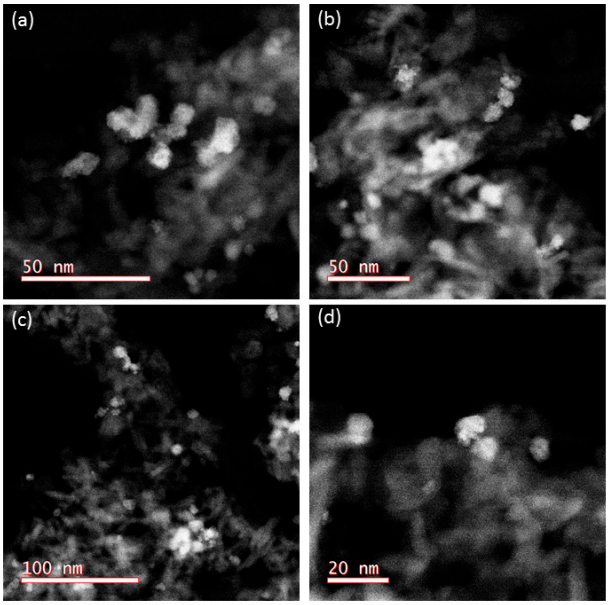

Figure 6. (**a**–**d**) Low-magnification HAADF STEM images show the PdO/PdO_x distributed in γ-Al_2O_3.

2.2.2. X-ray Photoelectron Spectroscopy (XPS)

XPS is widely used in catalytic research for identifying surface compounds and their composition [3,7,9,10]. An important objective of this research is to find out the change in surface composition of the catalyst before and after methane combustion and to identify the active phases in the catalytic reaction. We used the Pd 3d5/2 peak deconvolution technique to estimate the surface composition of the catalyst. The quality of the fit is good for XPS peaks, particularly with the very small signals of Pd observed and the "roughness" of nanoparticle specimens, which block a significant fraction of the outgoing photoelectron signal (smoother surfaces, such as Si, yield much higher S/N spectra). All of the XPS peak fits reported have chi-squared values <3.0. Further, there was no attempt to "guide" the peak fit to a preconceived surface chemistry. The peak fit was set to float freely in terms of binding energy, peak width, and combination of Gaussian/Lorentzian peak envelopes to model XPS peak shapes.

XPS of the catalyst gave a surface elemental composition of 0.37 atomic % Pd and 1.64 wt % of Pd. The catalyst contained 4.3 wt % Pd based on EDS data. This means that 35.8% of total Pd was on the surface and the rest of the Pd was in the bulk.

The binding energies (BE) for Pd 3d are 335.78 eV for Pd native oxide (PdO_x); 336.96 eV for PdO; and 338 eV for metallic Pd [25]. The vertical lines in the XPS Figure 7 identify the BE locations for standard, well-characterized Pd surface compounds [25]. PdO_x (Palladium native oxide) is designated as "PdNtv" in this research article. A high-resolution XPS spectrum (Figure 7) of the deconvoluted $Pd3d5_{/2}$ peak of the catalyst produced two distinct peaks with BE of 337 ev for PdO and 335.8 ev for PdNtv. The XPS data also confirmed the surface composition to be 38% PdO and 62% Pd native oxide. XPS did not show any peak for elemental Pd, thereby confirming the absence of metallic palladium in the catalyst. This result is in contrast to previous research reports on the presence of metallic Pd in Pd/γ-Al_2O_3 catalysts [18–20,26]. In addition to metallic Pd and stoichiometric PdO, palladium surfaces exhibit non-stoichiometric native oxides. Most native oxides are not stoichiometric and commonly designated as PdO_x. The bulk of a catalyst could be micro-structured with PdO while the surface composition exists as non-stoichiometric (native) palladium oxide [25]. The BE for Pd 3d5/2 peaks for a 3% PdO/γ-Al_2O_3 catalyst were in the range 335.2–336.8 ev and assigned to Pd and PdO; a peak with BE of 337.8 ev was due to PdO_2 [3] To the best our knowledge, this is the first research report for the presence of both PdO and Pd native oxide (PdO_x) on the surface of the supported catalyst

before reaction. In-situ XPS of a palladium catalyst on La-modified aluminum oxide confirmed PdO as the main surface compound in 'lean (oxygen rich)' conditions [27].

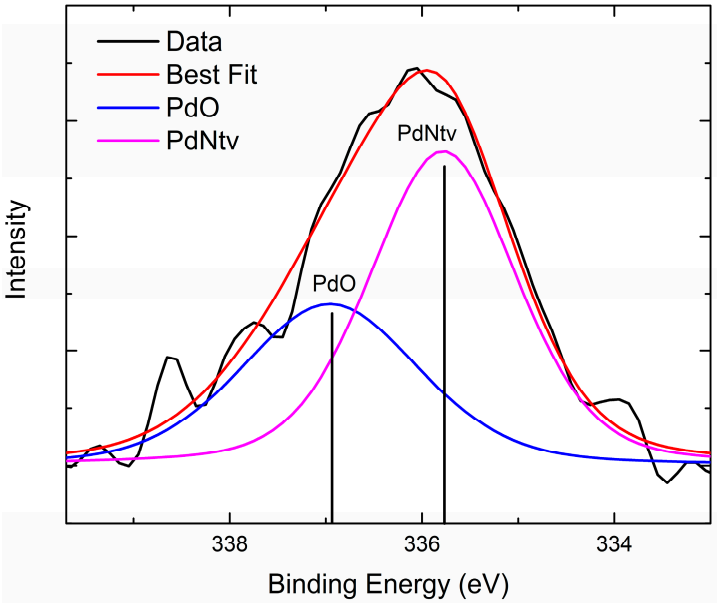

Figure 7. XPS (deconvoluted $3d_{5/2}$ peak) of the catalyst. PdNtv, Palladium native oxide.

2.2.3. X-ray Powder Diffraction

Figure 8 gives the XRD patterns of the catalyst, pure PdO, and γ-Al_2O_3. The important peaks for γ-Al_2O_3 are the peaks at 46.0° and 67.4° and the identifying peaks for PdO are a strong peak at 34.1° and smaller peaks at 42.2°, 54.9°, 61.1°, and 71.7°. The catalyst gave two weak XRD peaks at 34.1° (strongest peak for PdO) and 46.0° (strongest peak for γ-Al_2O_3), confirming the presence of PdO and γ-Al_2O_3. The catalyst as well as the standard PdO also showed an unexpected peak at 26.0°. This is due to graphite contamination originating from the carbon tape. The catalyst was in nanopowder form, and did not stick to the XRD sample plate. Hence, a carbon tape was used as an adhesive, and part of it remained in the sample during XRD. This contamination was much less during sample preparation of PdO; the gamma alumina support was sticking to the plate and hence no carbon tape was needed. Our XRD data were similar to reported values [3,4].

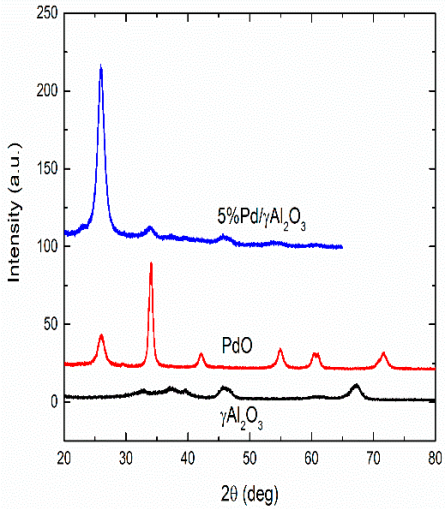

Figure 8. XRD of the catalyst, PdO, and the support.

2.2.4. Physisorption and Chemisorption

We used the Brunauer–Emmett–Teller (BET) method of nitrogen physisorption to calculate the total surface area; and Barrett-Joyner-Halenda (BJH) method to estimate pore volume and pore size of the catalyst. CO pulse chemisorption experiments provided data to calculate the dispersion and particle size (Crystallite size) of the catalyst. The calculations were done based on 5% Pd loading and chemisorption of one molecule of CO on each Pd atom on the surface. Table 1 gives the calculated physical and chemical properties of the catalysts. Our values of dispersion and particle size of the catalyst are similar to the data reported in the literature for $Pd/\gamma\text{-}Al_2O_3$ catalysts [3,4].

Table 1. Properties of the catalyst.

Properties	Values
BET Surface Area	147.7 m^2/g
BJH Pore Volume	0.615 cm^3/g
BJH Pore Size	13.7 nm
CO uptake in chemisorption	56.2 umol/g
Dispersion	14.0%
Metal surface area	2.66 m^2/g
Particle size	9.37 nm
Pd wt % [EDS]	4.3%

Figure 9 shows the temperature-programmed oxidation (TPO) profile of the $Pd/\gamma\text{-}Al_2O_3$ catalyst. The plot is noisy, displaying no definitive oxygen uptake. Miller et al. [20] reported a TPO peak around 286 °C due to the Pd-PdO transition. The more likely explanation of the plot's noise is that the surface already had a high content of PdO prior to the oxidation procedure, and hence oxygen update would be limited. Figure 10 displays the temperature-programmed reduction (TPR) profile for the catalyst. The TPR experiment was conducted without any prior reduction of the catalyst by hydrogen. As stated in the methods section, after pretreatment with helium, hydrogen gas was flown through the catalyst at 30 °C, and then the temperature was raised up to 500 °C. The TCD signals were recorded from 30 °C Hydrogen consumption to reduce PdO/PdO_x on the catalyst surface, which should happen at 0–30 °C as reported by Miller et al. [20]. However, this peak is missing in the TPD graph since measurements were started only from 30 °C. The TPD showed a peak around 60 °C and this is attributed to the decomposition of palladium hydride [20].

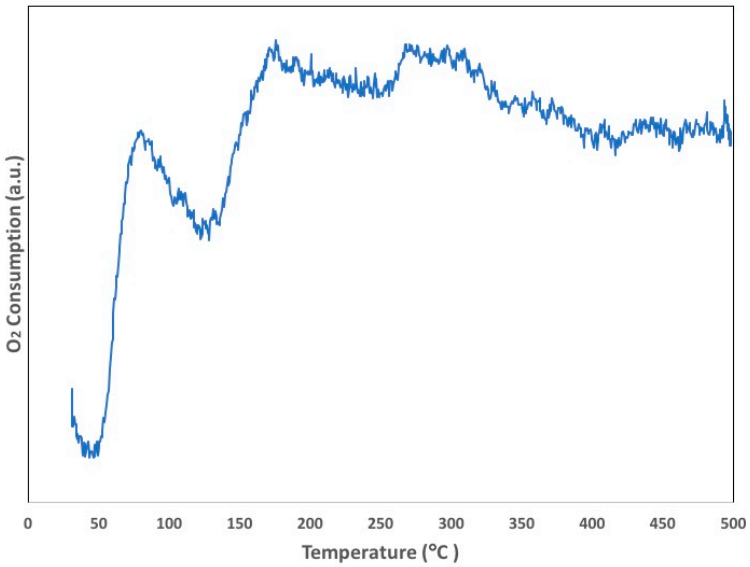

Figure 9. Temperature-programmed oxidation (TPO) of the catalyst.

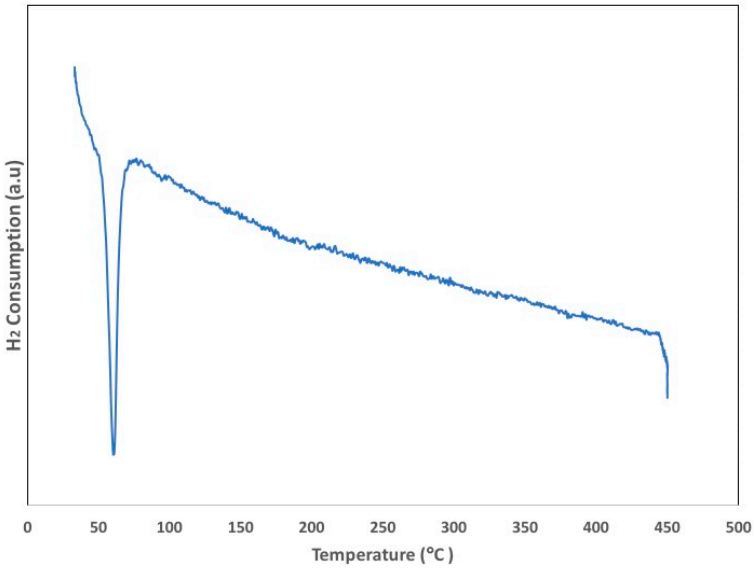

Figure 10. Temperature-programmed reduction (TPR) of the catalyst.

2.3. Activity Studies

The activity of the catalyst was tested with two separate reacting gas mixtures: (**a**) 1% methane, 4% oxygen, and balance helium; (**b**) 2% methane, 4% oxygen, and balance helium. The first gas mixture resembles a "lean-burn" condition, and the second one is the stoichiometric ratio for the catalytic combustion reaction. Each activity run was performed in a fixed reaction temperature for a reaction period of 20 min and a space velocity of 3.0×10^5 cc·g^{-1}·h^{-1}. Figure 11 gives the conversions of methane at different temperatures.

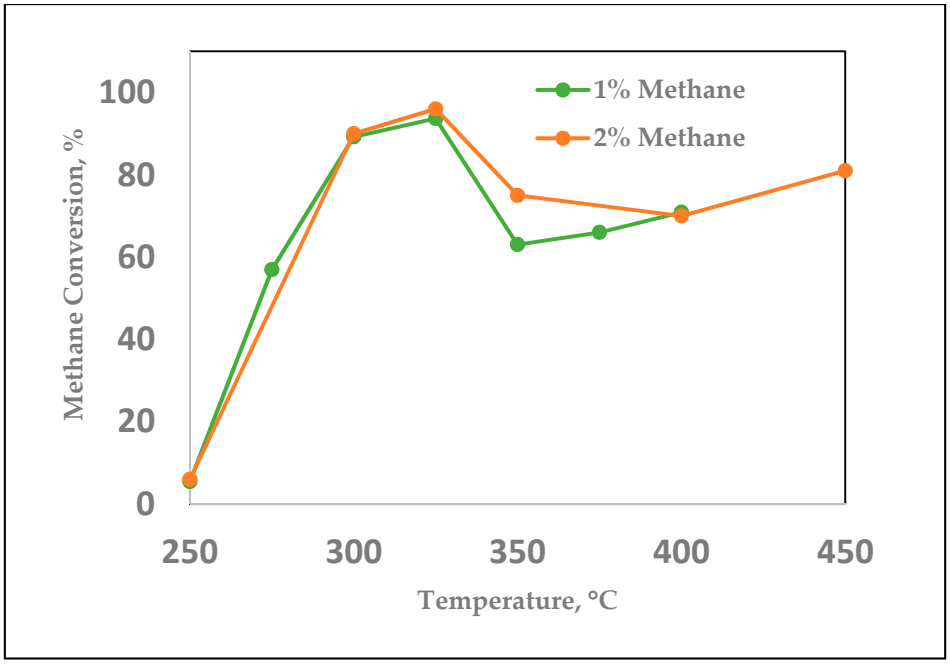

Figure 11. Activity of the catalyst at different temperatures.

The catalyst initiated combustion at 250 °C and attained 60% conversion at 275 °C and 90% at 300 °C with both gas mixtures. The highest conversion was 95% at 325 °C. All values of conversions

were between 90–94% in a narrow temperature range of 300–320 °C and we did not get 100% conversion under the experimental conditions. The reaction became very exothermic and water condensation was visible in the reactor in the narrow temperature range of 325 °C and above. The conversion of methane decreased from 95% to 70% for the 2% methane gas mixture as the temperature increased from 325 °C to 400 °C; the 1% gas mixture had a more pronounced dip in conversion in this temperature range. The catalytic reaction did not produce any carbon monoxide with the 1% and 2% methane gas mixtures.

An activity run with pure PdO was conducted in the catalytic reactor using a gas mixture of 1% methane, 4% oxygen, and balance helium. Methane conversion was 60% at 230 °C and 100% at 260 °C. In comparison, the 5% Pd/γ-Al_2O_3 catalyst could convert only 30% methane at 260 °C.

Table 2 gives a brief review of some promising catalysts developed in recent years. These catalysts showed high activities for methane conversion of 90% or more at 400 °C [3,7–9,11,28,29]. These catalysts have been developed using different preparation methods, such as Pd loading, and tested under different reaction conditions. Hence, it is not feasible to compare the relative effectiveness of these catalysts. However, among these catalysts, only two exhibited excellent low-temperature activity with a methane conversion of 90% and above at 325 °C. A Pd/Co_3O_4 on a ZrO_2 foam catalyst converted 90% of methane [8]. Our PdO-PdO_x catalyst converted 95% methane at 325 °C. The high methane conversion at low temperature is partly attributed to the vortex method providing better dispersion.

The efficiency and stability of the catalyst were tested on a preliminary basis by carrying out the catalytic reaction for six catalytic cycles under the best conversion conditions (at 320 °C for 20 min with 2% methane, 4% oxygen gas mixture, and a space velocity of 3.0 × 10^5 cc·g^{-1}·h^{-1}). The data in Table 3 show the catalyst was efficient in maintaining high conversion (90–94%) and was stable without much change in the surface composition after a reaction period of 2 h.

Table 2. Review of recent literature on catalytic activity for methane combustion.

Ref	Catalysts	Methane Conversion, %	
	(Metal loading, wt %)	325 °C	400 °C
[a]	5% Pd/γ-Al_2O_3	95	70
[8]	3% of Pd/Co_3O_4 on ZrO_2 foams	90	100
[11]	1% Pd on silicate monolith	80	100
[9]	1% Pd@CeO_2/γ-Al_2O_3	50	100
[28]	3% of Pd/Co_3O_4 on alumina foam	35	95
[29]	5% Pd/Co_3O_4	30	90
[3]	3% Pd/γ-Al_2O_3	30	90
[7]	0.05% Pd-Co/Al_2O_3	20	90

[a] This research report.

Table 3. Methane conversion in six catalytic cycles.

Run *	Methane Conversion, %
1	94
2	94
3	92
4	90
5	92
6	90

* 325 °C, 20 min; space velocity, 3.0 × 10^5 cc·g^{-1}·h^{-1}; 2% CH_4, 4%O_2.

The thermal stability of the catalyst was also tested by heating the catalyst up to 550 °C for 2 h in a flow of helium. XPS of the catalyst after the thermal treatment in a helium atmosphere did not show any change in the surface composition. XPS (Figure 12) of the catalyst after five reaction cycles indicated no change in the surface Pd content. However, there was a small change in the surface

composition of the catalyst (PdO, 49%; PdNtv oxide, 51%) compared to the original composition of the catalyst before reaction (PdO, 38%; PdNtv oxide, 62%).

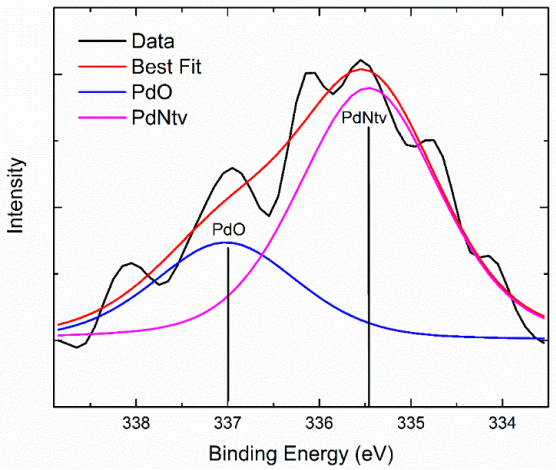

Figure 12. XPS (deconvoluted $3d_{5/2}$ peak) of the catalyst after five catalytic cycles.

Many researchers reported deactivation of catalysts by steam at higher temperatures (above 400 °C) resulting in sintering and or poisoning [6,15,16]. At temperatures above 325 °C, the conversion decreased, but the surface Pd content did not change (Table 4). The catalyst after reaction with 2% methane at 320 °C did not show any loss of surface Pd. This indicates that the catalyst was stable at lower temperatures up to 320 °C and was not deactivated by steam. It appears that deactivation by steam may not be the only reason for the decrease in catalytic activity at 325–450 °C.

Table 4. Change in surface composition with reaction conditions

Reaction Conditions	Surface Pd, wt %	Surface Composition, wt %	
		PdO	PdO_x
Catalyst before reaction (Figure 7)	1.64	38	62
Catalyst after reaction at 325 °C (Figure 12)	1.62	49	51
Catalyst after reaction at 450 °C (Figure 14)	1.62	68	32
Pd nitrate calcined at 500 °C (Figure 13)	-	100	0
Pure PdO before and after reaction	-	100	0

2.4. Active Phase of the Catalyst and Proposed Mechanism

Disputes exist on the active phases in methane catalytic combustion. Some researchers reported PdO as the active Pd species [2,6,7,9,27]. However, others attribute the highest catalytic activity to the Pd metallic state in methane-rich conditions [18,19,27] or to the ratio of Pd to PdO [20,21]. Another consideration is the possibility of the support itself lending its constituents to the catalytic active site during the course of the reaction [20]. For example, under some situations, oxygen from the aluminum oxide support could migrate to the palladium, forming PdO or some form of PdO_x, and/or migrate to the gas-phase molecule providing oxygen for the combustion [5,22].

In order to explore the support effect, we did XPS of standard PdO (Sigma Aldrich, St. Louis, MO, USA) before and after reaction with 2% methane and 4% oxygen gas mixture at 325 °C. The best-fit data indicated the presence of only 100% PdO with a binding energy of 336.96 ev in both XPS spectra. This indicates that PdO remained as the active phase in the catalytic reaction of methane with pure PdO without the support. Pd (II) nitrate was the precursor for the catalyst. Since the catalyst was prepared by calcination in air at 500 °C, we treated the precursor under the same conditions by calcining at 500 °C and then did the XPS of the calcined Pd (II) nitrate (Figure 13).

The best-fit data indicated the presence of 100% Pd in the calcined Pd (II) nitrate with a binding energy of 336.96 ev. XPS (Figure 7) of the supported catalyst confirmed the presence of PdO and Pd native oxides (PdO_x) and that the native oxide formed only in the presence of the support. The XPS of calcined Pd nitrate showed only PdO and no native oxide. This confirms the supposition that the γ-Al_2O_3 support facilitated oxygen migration from the support to the stoichiometric PdO to form Pd native oxide (PdO_x). Other researchers reported the presence of Pd and/or PdO in Pd/γ-Al_2O_3 catalysts [2,6,7,9,18,19]. Miller et al. [20] and Schwartz et al. [22] suggested that the support could facilitate oxygen mobility and affect composition of the surface catalytic sites at temperatures <400 °C.

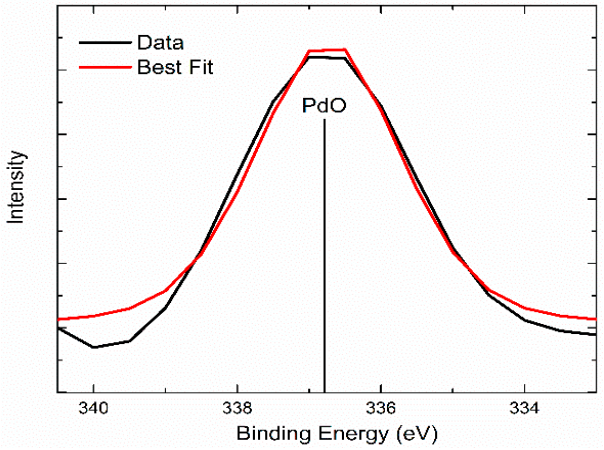

Figure 13. XPS ($Pd3d_{5/2}$ peak) of calcined Pd (II) nitrate.

In order to identify the active phases in the catalytic combustion process, we did XPS of the catalyst after reaction with 2% CH_4/4% O_2 at 450 °C for 20 min. XPS of the deconvoluted $3d_{5/2}$ peak gave a surface composition of 68% PdO and 32% Pd native oxide (Figure 14). Table 4 summarizes the surface composition at various reaction conditions based on XPS data. The evidences from XPS suggest that the surface composition of the catalyst changed after the reaction and the surface contained more PdO than Pd native oxide (PdO_x).

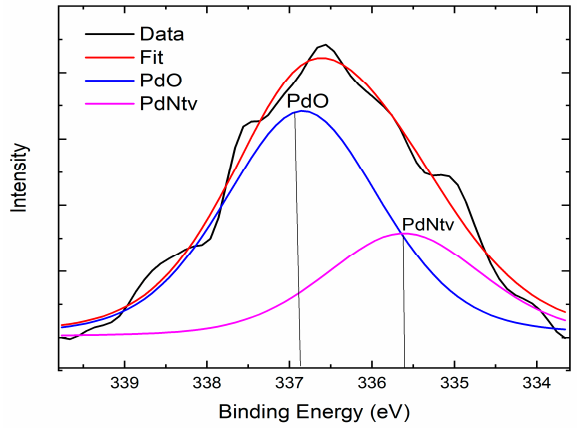

Figure 14. XPS (deconvoluted $Pd3d_{5/2}$ peak) of catalyst after reaction at 450 °C.

We are proposing the following hypotheses and tentative mechanism based on the experimental data:

(i) The active phase of the catalyst is Pd native oxide (PdO_x); during the catalyst preparation and calcination process, the oxide ions from the support, γ-Al_2O_3, migrate to PdO to form PdO_x. This mechanism supports the presence of both PdO and PdO_x in the catalyst before reaction.

(ii) During the reaction at lower temperatures below 325 °C, oxide ions from PdO_x migrate to react with methane; PdO_x forms PdO; and oxide ions from the support (γ-Al_2O_3) migrate to PdO to form PdO_x. This process maintains the surface composition of both PdO and PdO_x; the catalytic activity remains more or less steady since the active phase of PdO_x does not deplete.

(iii) At a higher temperature when catalytic activity decreases in the temperature range 325–450 °C, oxide ions from PdOx migrate to react with methane; and PdO_x forms PdO. However, due to unknown reasons (may be due to deactivation by steam) the support does not provide oxide ions to PdO and thereby the number of active sites of PdO_x decreases and hence activity decreases. This hypothesis supports the correlation between decrease in catalytic activity and depletion of PdO_x at temperatures in the range 325–400 °C as shown by XPS.

Based on isotope exchange evidences, Schwartz and Pfefferle [22] suggested that at temperatures below 350 °C, any oxygen exchange in reaction is due to oxygen from the support. Therefore, our results and suggested mechanism are in agreement with these researchers.

3. Materials and Methods

3.1. Catalyst Synthesis

We developed a modified Vortex-assisted Incipient Wetness Method to improve mixing and dispersion of the catalyst precursor in the support. The vortex unit is an *Analog Vortex Mixer with Single Tube Holder* (Fisher Scientific; Catalog number 02-215-430, Asheville, NC, USA). The vortex unit is given in Figure 15. The vortex mixer (bottom part) is attached to a tube holder that holds and secures a vortex tube. The solid support is taken in the vortex tube and the catalyst precursor solution is added to the support drop-by-drop. An analog controller controls the speed (0–3000 rpm), which allows for high-speed mixing for vigorous vortexing of samples.

Figure 15. Vortexing Unit.

A modified Vortex-assisted Incipient Wetness Method was developed to prepare a 5 wt % Pd/γ-Al_2O_3 catalyst. A solution of 3.0 mL deionized (DI) water and 0.328 g of palladium(II) nitrate hydrate (Sigma Aldrich, MW: 230.43 g/mol; anhydrous basis) was added in 20 µL increments to 2.702 g of gamma phase aluminum oxide nanopowder (<50 nm particle size, Sigma Aldrich, St. Louis, MO, USA) under vortex mixing set to 900 rpm for 2 h. The resulting "ball" of dough-like mixture was dried in an oven at 103 °C overnight, crushed with a mortar and pestle, and then calcined at 500 °C for 6 h in a *Thermolyne* Benchtop Muffle Furnace. This catalyst was then passed through a sieve to achieve a particle size of <150 µm.

Palladium oxide (99.97% trace metals basis, Sigma Aldrich, St. Louis, MO, USA) was used as a standard for the XPS, XRD, and catalytic activity tests.

3.2. Catalyst Characterization

Samples were characterized by X-ray photoelectron spectroscopy (XPS), physisorption, chemisorption, and temperature-programmed techniques, powder X-ray diffraction (XRD), and Scanning Transmission Electron Microscopy (STEM).

XPS measurements were conducted in a load-locked Kratos XSAM 800 (Kratos Analytic Ltd., Manchester, U.K.) surface analysis system equipped with a hemispherical energy analyzer and a MgK_α (1253.6 eV) radiation source and following a procedure reported earlier [30]. The C1s binding energy of 285.0 eV was used as the reference. The XPS data reported were run under two instrumental setups. For survey spectra (broad-spectrum cases), we scanned 20 times at an energy step of 0.5 eV. For the higher-resolution spectra where peak deconvolution was performed, we scanned only over the peak of interest with a varying number of scans (determined by the peak size) with a higher energy resolution step of 0.1 eV. All other instrumental parameters (X-ray flux, tilt angle, etc.) were the same.

X-ray analysis of the catalyst, standard PdO, and standard γ-Al_2O_3 was conducted in a *Bruker AXS D2 Phaser* using a Cu radiation source at 30 kV and 10 mA. Samples were irradiated at a 2 range from 15 to 90° at a speed of 2.4°/min. Samples were either applied to a zero-plate or to double-sided tape to ensure even application to the XRD slide.

Chemisorption measurements were performed in a Micromeritics AutoChem II 2920 (Micromeritics Corporation, Norcross, GA, USA) and details of the procedure have been reported [20,31]. For the pulse chemisorption experiment, the catalyst was first reduced in hydrogen at 450 °C and then pulses of CO were injected. Dispersion and particle size (Crystallite size) of the catalyst were calculated from the CO uptake, wt % of Pd loading, and assuming a 1:1 ratio between the CO-adsorbed and Pd-active site. The temperature-programmed reduction (TPR) experiment involved pretreatment by helium at 110 °C followed by a flow of 10% H_2/Ar at 30 °C and then continuing heating up to 500 °C in a flow of 10% H_2/Ar. For the TPO experiment, the TPR procedure was followed except using 10% O_2/He instead of H_2/Ar. The physisorption experiment was performed in a Micromeritics TriStar II 3020 3.02 (Micromeritics Corporation, Norcross, GA, USA) surface and porosity analyzer using nitrogen gas as adsorbate at minus 198.8 °C. Surface area was calculated using the BET method; the pore volume from the BJH adsorption cumulative volume of pores between 17,000 Å and 3,000,000 Å width; and the pore size from the BJH adsorption average pore width (4V/A).

HAADF-STEM images and EDS elementary mapping were obtained in a *Hitachi HD2700* (Hitachi Ltd., Tokyo, Japan) aberration-corrected scanning transmission electron microscope. The electron beam convergent angle α was ~27 mrad and the HAADF detector collection angle β = 70–370 mrad.

3.3. Activity Measurements

The catalytic activity measurements were performed in a temperature-controlled tubular fixed-bed quartz reactor. A catalyst bed of 0.200 g was secured in the middle of the reactor by quartz wool/beads. Helium gas (1.0 L/min) was passed through the catalytic reactor and the reactor temperature was raised to a desired value by a temperature-controlled furnace. The temperature of the reaction bed

was measured by a thermocouple connected to a digital temperature recorder. The flow of helium was stopped when the desired temperature in the reaction bed was established. A certified gas mixture (for example: 1% methane, 4% oxygen, balance helium; Airgas certified) passed through an automatic *mass flow controller* (Aalborg, GFC17, Aalborg, Orangeburg, NY, USA) at a flow rate of 1.0 L/min and then to the catalyst bed. The effluent gas mixture (carbon dioxide, water vapor, unreacted methane, oxygen, and helium) from the reactor passed through a moisture trap and a tee junction fitted with a septum. The effluent gas mixture was collected in a gas-tight syringe (*Restek*) by inserting the syringe into the septum. An amount of 1.0 cc of the sampled effluent gas mixture was injected into a gas chromatograph (Buck Scientific Model 310, Buck Scientific Inc., Norwalk, Connecticut, USA) fitted with a 6 ft. *shincarbon* packed column and a Thermal Conductivity Detector (TCD). The GC data was analyzed using *PeakSimple* software to determine the peak area and a calibration chart to calculate the % by volume of methane and carbon dioxide.

A preliminary assessment of the efficiency and stability of the catalyst was performed by repeating a catalytic activity run six times under the same reaction conditions (320 °C for 20 min with 2% methane, 4% oxygen gas mixture, and a space velocity of 3.0×10^5 cc·g^{-1}·h^{-1}). Each catalytic cycle run had the following sequence: (a) He was passed through the reactor containing 0.2 g of catalyst in the bed; (b) the temperature of the bed was raised to 325 °C while passing helium; (c) the helium flow was stopped and the reacting gas mixture (2% methane, 4% oxygen, balance helium) was passed through the reactor while maintaining the bed temperature at 325 °C; (d) after 20 minutes, a sample of the product gas mixture was collected and injected to the gas chromatograph; and (e) the reaction gas mixture flow was discontinued and the helium flow continued while the reactor was cooled down to room temperature. The next catalytic cycle run had all of the five steps of the first run while keeping the original catalyst in the bed intact.

The conversion of methane was calculated using the following equation:

$$\text{Conversion}(\%) = \frac{[CH_4]_{in} - [CH_4]_{out}}{[CH_4]_{in}} \times 100\%.$$

4. Conclusions

A PdO-PdO_x/γ-Al_2O_3 catalyst was prepared by a modified Vortex-assisted incipient Wetness Method. The catalyst had 4.3% Pd as total Pd content and a surface composition of 38% PdO and 62% Pd native oxide (PdO_x). HAADF-STEM images revealed PdO_x nanocrystals of 5–10 nm sizes; y-Al_2O_3 particles were crystalline and not amorphous; and PdO_x particles were distributed in the support. The catalyst was effective in achieving a high conversion of 95% at 325 °C and the conversion was within 90–94% in a narrow temperature range of 300–320 °C. The catalyst displayed high efficiency and thermal stability at and below 325 °C and was not deactivated by steam. However, the catalytic activity decreased above 325 °C and came down to 70% at 400 °C. Our catalyst works well only in a narrow low-temperature range of 300–320 °C. The high methane conversion at low temperature is attributed to the vortex method providing better dispersion and to catalyst–support interaction producing the active phase of PdO_x. Future research would include improvement of this catalyst, exploring its viability in real "lean-burn" conditions, and testing our hypotheses and proposed mechanism. The results of this research are consistent with the works of Miller et al. [20] and Schwartz et al. [22] highlighting the roles of PdO and PdO_x in the combustion of methane at low temperatures, and corroborating that alumina as a support material stabilizes the PdNtv species and facilitates oxygen migration.

Author Contributions: A.C.B. provided the concept and guidance for this research and did the writing as the corresponding author; J.M.M. did the equipment design, methods, catalyst preparation, activity runs, and XRD; O.L. performed the catalytic cycle runs and repetitions of activity runs; M.J.B. performed all XPS experiments and data interpretation.

Funding: This research received no external funding.

Acknowledgments: This research was partly funded by Columbus State University Research Grants to A.B and SRACE grants to J.M. and O.L. We thank (a) Yong Ding and Todd Walters of the Georgia Tech Materials Characterization Facility for STEM and EDS images and interpretations; (b) Taylor Sulmonetti, *Christopher W. Jones Research Group*, Georgia Institute of Technology for adsorption experiments; and (c) D.W. Holley of Columbus State University for reading and editing the manuscript.

Conflicts of Interest: The authors declare no conflicts of interest.

References

1. Farrauto, R.J. Low-temperature oxidation of methane. *Science* **2012**, *337*, 659–660. [CrossRef] [PubMed]
2. Gélin, P.; Primet, M. Complete oxidation of methane at low temperature over noble metal based catalysts: A review. *Appl. Catal. B Environ.* **2002**, *39*, 1–37. [CrossRef]
3. Simplício, L.M.T.; Brandão, S.T.; Sales, E.A.; Lietti, L.; Bozon-Verduraz, F. Methane combustion over pdo-alumina catalysts: The effect of palladium precursors. *Appl. Catal. B Environ.* **2006**, *63*, 9–14. [CrossRef]
4. Yoshida, H.; Nakajima, T.; Yazawa, Y.; Hattori, T. Support effect on methane combustion over palladium catalysts. *Appl. Catal. B Environ.* **2007**, *71*, 70–79. [CrossRef]
5. Gholami, R.; Smith, K.J. Activity of pdo/SiO_2 catalysts for Ch_4 oxidation following thermal treatments. *Appl. Catal. B Environ.* **2015**, *168–169*, 156–163. [CrossRef]
6. Goodman, E.D.; Dai, S.; Yang, A.-C.; Wrasman, C.J.; Gallo, A.; Bare, S.R.; Hoffman, A.S.; Jaramillo, T.F.; Graham, G.W.; Pan, X.; et al. Uniform pt/pd bimetallic nanocrystals demonstrate platinum effect on palladium methane combustion activity and stability. *ACS Catal.* **2017**, *7*, 4372–4380. [CrossRef]
7. Stefanov, P.; Todorova, S.; Naydenov, A.; Tzaneva, B.; Kolev, H.; Atanasova, G.; Stoyanova, D.; Karakirova, Y.; Aleksieva, K. On the development of active and stable pd–co/γ-Al_2O_3 catalyst for complete oxidation of methane. *Chem. Eng. J.* **2015**, *266*, 329–338. [CrossRef]
8. Ercolino, G.; Stelmachowski, P.; Specchia, S. Catalytic performance of pd/Co_3O_4 on sic and ZrO_2 open cell foams for process intensification of methane combustion in lean conditions. *Ind. Eng. Chem. Res.* **2017**, *56*, 6625–6636. [CrossRef]
9. Cargnello, M.; Delgado Jaen, J.J.; Hernandez Garrido, J.C.; Bakhmutsky, K.; Montini, T.; Calvino Gamez, J.J.; Gorte, R.J.; Fornasiero, P. Exceptional activity for methane combustion over modular pd@CeO_2 subunits on functionalized Al_2O_3. *Science* **2012**, *337*, 713–717. [CrossRef] [PubMed]
10. Khader, M.; Al-Marri, M.; Ali, S.; Abdelmoneim, A. Active and stable methane oxidation nano-catalyst with highly-ionized palladium species prepared by solution combustion synthesis. *Catalysts* **2018**, *8*, 66. [CrossRef]
11. Xiao, C.; Yang, Y.; Meng, D.; Dong, L.; Luo, L.; Tan, Z. Stable and active monolithic palladium catalyst for catalytic oxidation of methane using nanozeolite silicalite-1 coating on cordierite. *Appl. Catal. A Gen.* **2017**, *531*, 197–202. [CrossRef]
12. Li, M.; Gui, P.; Zheng, L.; Li, J.; Xue, G.; Liang, J. Active component migration and catalytic properties of nitrogen modified composite catalytic materials. *Catalysts* **2018**, *8*, 125. [CrossRef]
13. Zhang, X.; Long, E.; Li, Y.; Zhang, L.; Guo, J.; Gong, M.; Chen, Y. The effect of CeO_2 and bao on pd catalysts used for lean-burn natural gas vehicles. *J. Mol. Catal. A Chem.* **2009**, *308*, 73–78. [CrossRef]
14. Venezia, A.M.; La Parola, V.; Liotta, L.F. Structural and surface properties of heterogeneous catalysts: Nature of the oxide carrier and supported particle size effects. *Catal. Today* **2017**, *285*, 114–124. [CrossRef]
15. Farrauto, R.J.; Hobson, M.C.; Kennelly, T.; Waterman, E.M. Catalytic chemistry of supported palladium for combustion of methane. *Appl. Catal. A Gen.* **1992**, *81*, 227–237. [CrossRef]
16. Chin, Y.-H.; Buda, C.; Neurock, M.; Iglesia, E. Consequences of metal–oxide interconversion for c–h bond activation during CH_4 reactions on pd catalysts. *J. Am. Chem. Soc.* **2013**, *135*, 15425–15442. [CrossRef] [PubMed]
17. Gholami, R.; Alyani, M.; Smith, K. Deactivation of pd catalysts by water during low temperature methane oxidation relevant to natural gas vehicle converters. *Catalysts* **2015**, *5*, 561. [CrossRef]
18. Sadokhina, N.; Ghasempour, F.; Auvray, X.; Smedler, G.; Nylén, U.; Olofsson, M.; Olsson, L. An experimental and kinetic modelling study for methane oxidation over pd-based catalyst: Inhibition by water. *Catal. Lett.* **2017**, *147*, 2360–2371. [CrossRef]
19. Bychkov, V.Y.; Tyulenin, Y.P.; Gorenberg, A.Y.; Sokolov, S.; Korchak, V.N. Evolution of pd catalyst structure and activity during catalytic oxidation of methane and ethane. *Appl. Catal. A Gen.* **2014**, *485*, 1–9. [CrossRef]

20. Miller, J.B.; Malatpure, M. Pd catalysts for total oxidation of methane: Support effects. *Appl. Catal. A Gen.* **2015**, *495*, 54–62. [CrossRef]
21. Kinnunen, N.M.; Hirvi, J.T.; Venäläinen, T.; Suvanto, M.; Pakkanen, T.A. Procedure to tailor activity of methane combustion catalyst: Relation between pd/pdox active sites and methane oxidation activity. *Appl. Catal. A Gen.* **2011**, *397*, 54–61. [CrossRef]
22. Schwartz, W.R.; Pfefferle, L.D. Combustion of methane over palladium-based catalysts: Support interactions. *J. Phys. Chem. C* **2012**, *116*, 8571–8578. [CrossRef]
23. Zhao, M.; Florin, N.H.; Harris, A.T. Mesoporous supported cobalt catalysts for enhanced hydrogen production during cellulose decomposition. *Appl. Catal. B Environ.* **2010**, *97*, 142–150. [CrossRef]
24. Vasilev, M.P.; Abiev, R.S. Dispersion of carbon nanotubes clusters in pulsating and vortex in-line apparatuses. *Chem. Eng. Sci.* **2017**, *171*, 204–217. [CrossRef]
25. Crist, B.V. *Handbook of Monochromatic Xps Spectra. The Elements of Native Oxides*; Wiley-VCH: Weinheim, Germany, 2000; ISBN 0-471-49265-5.
26. Xiong, H.; Wiebenga, M.H.; Carrillo, C.; Gaudet, J.R.; Pham, H.N.; Kunwar, D.; Oh, S.H.; Qi, G.; Kim, C.H.; Datye, A.K. Design considerations for low-temperature hydrocarbon oxidation reactions on pd based catalysts. *Appl. Catal. B Environ.* **2018**, *236*, 436–444. [CrossRef]
27. Huang, F.; Chen, J.; Hu, W.; Li, G.; Wu, Y.; Yuan, S.; Zhong, L.; Chen, Y. Pd or pdo: Catalytic active site of methane oxidation operated close to stoichiometric air-to-fuel for natural gas vehicles. *Appl. Catal. B Environ.* **2017**, *219*, 73–81. [CrossRef]
28. Ercolino, G.; Karimi, S.; Stelmachowski, P.; Specchia, S. Catalytic combustion of residual methane on alumina monoliths and open cell foams coated with Pd/Co_3O_4. *Chem. Eng. J.* **2017**, *326*, 339–349. [CrossRef]
29. Ercolino, G.; Stelmachowski, P.; Grzybek, G.; Kotarba, A.; Specchia, S. Optimization of pd catalysts supported on Co_3O_4 for low-temperature lean combustion of residual methane. *Appl. Catal. B Environ.* **2017**, *206*, 712–725. [CrossRef]
30. Duggan, J.N.; Bozack, M.J.; Roberts, C.B. The synthesis and arrested oxidation of amorphous cobalt nanoparticles using dmso as a functional solvent. *J. Nanopart. Res.* **2013**, *15*, 2089. [CrossRef]
31. Sulmonetti, T.P.; Pang, S.H.; Claure, M.T.; Lee, S.; Cullen, D.A.; Agrawal, P.K.; Jones, C.W. Vapor phase hydrogenation of furfural over nickel mixed metal oxide catalysts derived from layered double hydroxides. *Appl. Catal. A Gen.* **2016**, *517*, 187–195. [CrossRef]

© 2018 by the authors. Licensee MDPI, Basel, Switzerland. This article is an open access article distributed under the terms and conditions of the Creative Commons Attribution (CC BY) license (http://creativecommons.org/licenses/by/4.0/).